remote sensing

MDPI

Article

Tracking Deforestation, Drought, and Fire Occurrence in Kutai National Park, Indonesia

Ryan Guild [1,2], Xiuquan Wang [1,2,*] and Anne E. Russon [3]

[1] Canadian Centre for Climate Change and Adaptation, University of Prince Edward Island, St. Peters Bay, PE C0A 2A0, Canada
[2] School of Climate Change and Adaptation, University of Prince Edward Island, Charlottetown, PE C1A 4P3, Canada
[3] Psychology Department, Glendon College of York University, North York, ON M4N 3M6, Canada
* Correspondence: xxwang@upei.ca; Tel.:+1-902-739-2244

Abstract: The dry lowland and mangrove forests of Kutai National Park (KNP) in Indonesia provide invaluable ecosystem services to local human populations (>200,000 in number), serve as immense carbon sinks to recapture anthropogenic emissions, and safeguard habitats for thousands of wildlife species including the critically endangered Northeast Bornean orangutan (*Pongo pygmaeus morio*). With recent reports of ongoing illegal logging and large-scale wildfires within this National Park, we sought to leverage the extensive catalogue and processing power of Google Earth Engine to track the rates and influences of forest loss within KNP over various time periods since 1997. We present estimates of forest loss from the Hansen Global Forest Change v1.9 dataset (2000–2021) which detected a loss of 15% (272 km^2) of forest cover within KNP since 2000, half of which (137 km^2) coincided with the El Niño-induced wildfires of 2015–2016. Using the MCD64A1 C6.1 MODIS dataset, we found significant spatial overlap between burned area and forest loss detections during the 2015–2016 period but identified considerable omissions in the burned area dataset over smallholder farms within KNP. We discuss the implications of deforestation in areas of primary orangutan habitat and how patterns of forest loss have influenced drought and fire dynamics within KNP. Finally, we compare time-series estimates of precipitation, the ENSO index, burned area, and forest loss to demonstrate that fire risk within KNP depends largely—but not exclusively—on drought severity, and that rates of non-fire (gradual) and fire-related (extreme) forest loss threaten the remaining forests of this National Park.

Keywords: deforestation; wildfire; drought; satellite; Kutai National Park; Google Earth Engine

Citation: Guild, R.; Wang, X.; Russon, A.E. Tracking Deforestation, Drought, and Fire Occurrence in Kutai National Park, Indonesia. *Remote Sens.* **2022**, *14*, 5630. https://doi.org/10.3390/rs14225630

Academic Editor: Sandra Eckert

Received: 13 October 2022
Accepted: 5 November 2022
Published: 8 November 2022

1. Introduction

Kutai National Park (KNP) represents one of the last relatively intact areas of protected lowland and mangrove forest of Indonesian Borneo (Kalimantan) [1]. This protected area is home to over 300 species of birds, a significant population of the critically endangered Northeast Bornean orangutan (*Pongo pygmaeus morio*), and some of the last tracts of ecologically significant and commercially valuable Bornean ironwood trees in the region [1,2]. In addition to catastrophic wildfires reported during the extreme El Niño droughts of 1983–1984, 1997–1998 and 2015–2016 [3,4], KNP has continuously experienced illegal logging from nearby human populations for timber, expanding agricultural fields, and land speculation which the National Park authority struggles to address [5,6].

The use of high resolution (<30 m) multiband satellite imagery in such fields for ecosystem monitoring and biodiversity conservation has kept pace with gradual improvements in its access and availability [7]; today, it represents the primary resource by which researchers track changes in forest cover over time. Yet only two studies have attempted to track the extent of forest loss within KNP using satellite imagery. [5] first used visual inspection of Landsat imagery to detect areas of loss between 1990 and 2007 over KNP,

while [8] used supervised classification of Landsat imagery to detect forest loss in the eastern (populated) region of the park between 2006 and 2009. The latter study estimated an annual deforestation rate of 2.15% in the park's eastern region and attributed much of it to conversion to settlements and agricultural land. At this rate, complete loss of forest in the eastern half of KNP would occur by the mid-century; however, plans to relocate the capital city of Indonesia from Java to East Kalimantan by 2024 are likely to intensify pressures on KNP's forests and accelerate this time frame. This would represent a substantial loss to both the *morio* orangutan habitat within Indonesia and to the ecosystem services upon which local residents—more than 200,000 people within and immediately surrounding KNP—rely for fresh water, forest resources, and tourism (see [9]). Thus, an updated analysis of the rates, extents, and causes of forest loss within KNP using modern sensing and processing technologies is imperative.

The objective of this study is to track forest loss, drought, and fires over the past two decades in KNP using historical collections of thermal and spectral satellite imagery mostly sourced from Google Earth Engine (GEE). Specifically, we utilize the Hansen Global Forest Change (v1.9) dataset to track annual forest loss (2000–2021); the MODIS MCD64A1 C6.1 product to track fire-affected areas (2002–2021); and the CHIRPS (Climate Hazard InfraRed Precipitation with Stations) Pentad dataset to track drought patterns within KNP (1997–2021). We attempt to validate each of these using the appropriate data and methods. The data presented here provide information to researchers and governments to demarcate vulnerable areas of protected forests and to devise strategies to avert future forest loss in this National Park.

2. Data and Methods

2.1. Study Area

KNP covers 1927 km^2 along the eastern coast of Borneo in the Indonesian province of East Kalimantan (Figure 1) [9]. The ecology of the region comprises inland areas of primary and secondary lowland forests (<250 m above sea level) dominated by Dipterocarpaceae and Lauraceae family trees and coastal areas featuring mangrove forests and brackish estuaries [9]. KNP is bounded by two cities at its southeastern (Bontang) and northeastern (Sangatta) corners (Figure 1) that have each seen considerable population expansion since the park's formal declaration in 1995, which has prompted the excision of several illegally settled areas from KNP's formal boundaries [10]. The Sangatta River forms part of KNP's eastern and northern boundaries, while the remaining northern, western, and southern perimeters abut a contiguous series of industrial concessions, including an open-pit coal mine, plus wood fibre, timber, and oil palm plantations (Figure 1). Several small villages of a few thousand people remain within the bounds of KNP in the eastern and coastal areas [9] where many active and abandoned smallholder farms dominate the landscape (pers. obs.). Oil palm monocultures represent a large portion of planted agriculture within KNP primarily because of the high returns on land and labour afforded by the crop [11]. Encouragement by the Indonesian government to cultivate oil palms as a poverty-reduction strategy and growing contracts offered by palm oil companies in the region [12,13] have further incentivized farmers to illegally establish and enlarge oil palm plantations throughout eastern KNP.

In an intact old-growth state prior to 1970, the forests of KNP rarely experienced wildfires due to low combinations of fire hazards (i.e., dryness and fuel loads) and fire risks (i.e., prevalence of ignition sources) [14]. While ignition sources including lightning, swidden agriculture, and burning coal seam have existed in this region for millenia, neither naturally nor human-induced fires are believed to have driven large-scale deforestation here prior to 1970 [14,15]. However, fire hazards in this region have since increased from more frequent extreme droughts and unprecedented amounts of logging-related fuel loads, as have fire risks from the proliferation of croplands that use fire for various purposes (see [6]). Over the past 40 years, three super El Niño droughts have facilitated the spread of wildfires throughout KNP's forests. In 1982/83, around half of the park's forests burned [16] and

high mortality rates were reported for canopy trees, figs, and lianas [17], while in 1997/98, a much larger extent of the park burned and most of its forests were reset to a secondary successional stage [4,18]. The mixed-dipterocarp forests of this region can recover their structure when left undisturbed for a period of 10–20 years [19,20]. Most recently, during the super El Niño drought of 2015/16, island-wide studies revealed a significant number of fire detections over KNP [3,21], but the extent of—and damage caused by—burning during this event is yet unknown.

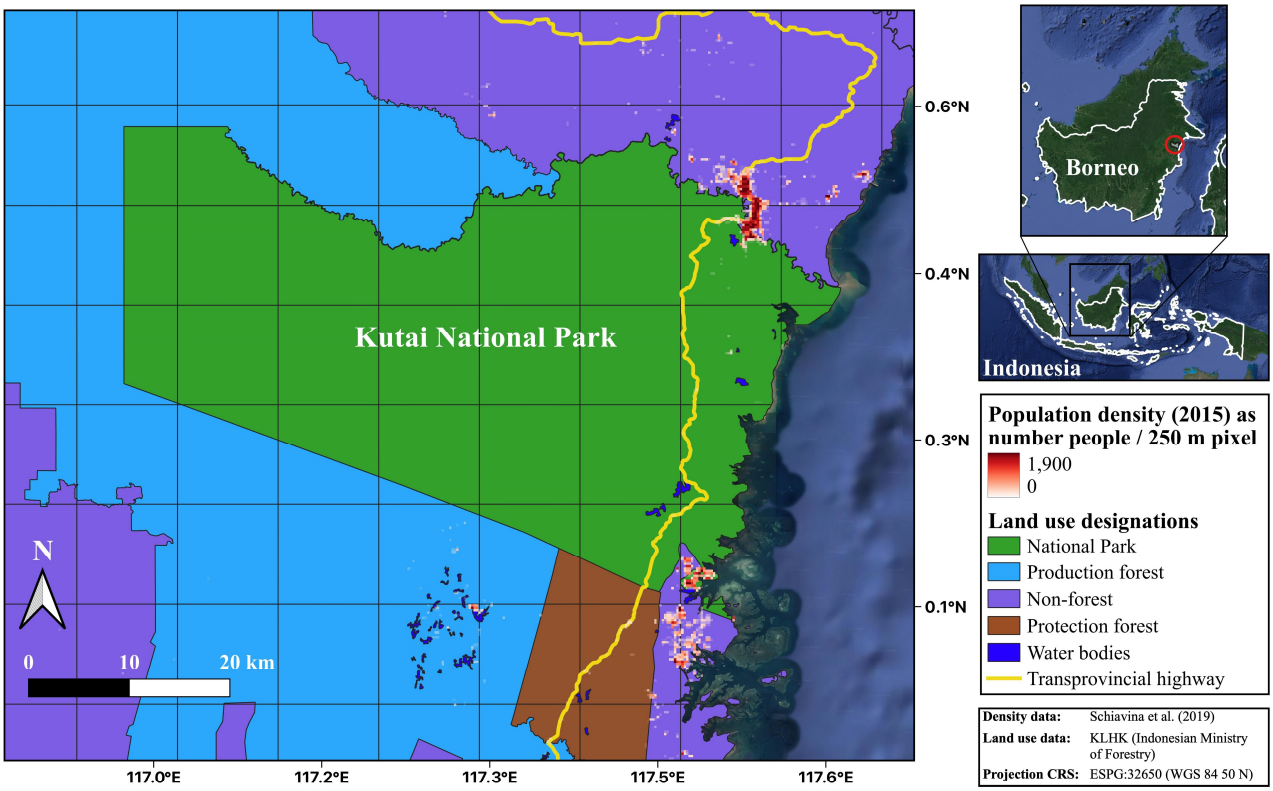

Figure 1. Land use designations and population density within and around Kutai National Park of East Kalimantan, Indonesia. Density displayed as estimated number of people per 250 m × 250 m grid cell [22] Southeastern and northeastern population centers represent the respective cities of Bontang and Sangatta.

2.2. Datasets

2.2.1. Hansen Global Forest Change (HGFC)

The HGFC v1.9 dataset is a global gridded (30 m) forest loss product available on GEE that uses a time-series change detection analysis of multispectral Landsat TM (L4 and L5), ETM+ (L7), and OLI/TIRS (L8) scenes to track annual changes in global forest cover between 2000 and 2021 [23,24]. The first release of the dataset (2000–2012) reported a producer's accuracy of 83.1% (overall accuracy 99.5%) over tropical domains [23]. The most recent version (v1.9) reports an improved detection accuracy since 2013 due to the inclusion of L8 data; thus, we only discretize post-2013 years annually in our analyses. Forest loss in HGFC is defined as a stand-replacement disturbance [of tree canopy cover] via removals or mortality and it uses a detection algorithm described by [24,25]. This dataset does not account for potential regrowth after a pixel has been assigned as 'lost', which prevents discernment of outcomes of canopy loss (i.e., regrowth, further degradation, conversion to other land uses) in our study area. Although high-resolution satellite imagery indicates that conversion to settlements and croplands predominate these outcomes over the frontline [loss] areas of eastern KNP, additional data and analysis is required to quantify the capacity for—and extents of—regrowth following canopy loss in our study area.

The 'treecover2000' and 'lossYear' bands of HGFC v1.9 contain classified pixels of (1) global tree canopy cover (vegetation >5 m in height) in the year 2000 (baseline) and (2) annual canopy loss between this baseline and 2021, respectively. We clipped these bands to the boundary of KNP, reduced them to area estimates using GEE functions, and exported them for colour rendering in QGIS. The full script (see Data Availability Statement) used to generate the raster images of annual forest loss in KNP was co-opted from a Google-based Earth Engine tutorial (https://developers.google.com/earth-engine/tutorials/tutorial_forest_02, accessed on 1 September 2022).

We employ two additional datasets to validate HGFC-detected areas of forest canopy loss over two sample regions within KNP between 2017–2020. First, we utilize the novel GEE-based Forest Canopy Disturbance Monitoring (FCDM) Tool using the developer-recommended parameter values to detect annual canopy loss within the sample regions. The FCDM Tool detects new canopy openings from L8 scenes across user-defined time periods and reports an overall accuracy of 77.8% within tropical evergreen rainforests [26]. Second, we visually inspected high-resolution (5 m) cloud-free composite images (June–November) via Planet/NICFI on GEE to manually delineate canopy loss over the sample regions for each year of the validation period. For this "reference" dataset (as referred to in this study), we first traced the extent of non-forest areas in the 2016 composite over both sample regions, then overlayed composites from each subsequent year to trace additional areas of canopy loss. Since each dataset uses a different temporal approach to detect canopy loss between years (see Figure A1), we focus our comparison on the total—rather than annual-extent(s) of detected forest loss between datasets.

2.2.2. MCD64A1 Burned Area

The MCD64A1 C6.1 burned area (BA) product (500 m) contains estimates of global monthly BA based on a time-series detection analysis of daily MODIS C6.1 observations between 07/2000 to 02/2022 [27]. Its most recent version (C6.1) reports an improved detection accuracy of BA (63% producer's; 97% overall), yet it still performs poorly over croplands due to spectral confusion between burnt and harvested land and a limited ability to detect small-burning fires [27–29]. We first generated annual mosaics of BA detections within KNP between 2002–2021 in GEE (see Data Availability and Source Code), and then colour-rendered and reduced each mosaic to area estimates (using the GRASS r.series algorithm) in QGIS. Using active fire (AF) observations from NASA's VIIRS (Variable Infrared Imaging Radiometer Suite) product (375 m) we graphed annual aggregates of daily fire counts within KNP (2012–2021) and compared the location of AF and BA detections during the wildfire years of 2015–2016. While the two datasets detect different signals of fire activity—thermal (AF) vs. post-fire burn scars (BA)—the AF (VIIRS) product can detect relatively smaller fires and is less susceptible to harvest-related confusion, making it valuable to compare against BA detections over cropland regions [30,31].

We attempted to validate the MCD64A1 dataset for the 2015 wildfires within KNP following the burn severity mapping approach developed by UN-SPIDER (United Nations Space-based Information for Disaster Management and Emergency Response). We first selected two sample areas of detected BA and determined the estimated date(s) of burning for each according to MCD64A1 and VIIRS datasets. We also selected one 'unburned' sample area (without BA detections) over SW KNP where numerous AF were detected in 2015. In GEE, we (1) generated cloud-free pre- and post-fire composite images over each sample region using L8 scenes, (2) calculated the normalized burn ratio (NBR) of each composite, and (3) produced a differenced normalized burn ratio (dNBR) image to classify burn severity for each of the three sample regions (see Data Availability Statement). We classified dNBR images using the burn severity thresholds and colour coding developed by the USGS (United States Geological Survey) and UN-SPIDER, respectively, and compared the classified images against the MCD64A1-detected burned areas over each sample region.

We chose to generate cloud-masked composite scenes of pre- and post-fire conditions to address the challenge of year-round high cloud cover that obscures most satellite scenes over KNP. This approach is not recommended given the potential for signal interference

over the composited time-period (e.g., through changes in vegetation greenness, agricultural harvests, etc.). However, our approach detected signals of browned (i.e., burnt) areas that are uncommon in scenes or composites from non-wildfire years over this region, and thus this offers value to our analysis of BA in KNP.

2.2.3. Climate Hazard InfraRed Precipitation and Station (CHIRPS)

The CHIRPS Pentad reanalysis gridded rainfall dataset combines infrared measurements of Cold Cloud Duration taken every 5 days (from the Tropical Rainfall Measuring Mission Multisatellite Precipitation Analysis) with in situ weather station data sourced from the World Meteorological Organization's Global Telecommunication System [32]. This global dataset has a spatial resolution of 5.5 km and is available from January 1981 to present.

To generate a time series of monthly rainfall estimates, we first used a GEE mapping function to calculate total monthly precipitation (mm) per pixel across KNP for each year between 2002–2021 (date range of MCD64A1 data), then averaged the pixel estimates across KNP for each month using a reducer function (see Data Availability Statement). Monthly estimates were exported from GEE as csv files and transformed into rolling three-monthly total precipitation (e.g., DJF, JFM, FMA, etc.) to reduce monthly variation and to better reflect medium-term drought conditions (cf. [33]). To evaluate spatial variations in rainfall patterns, we also mapped the 25-year (1997–2021) average of total fire-season (Aug–Nov) rainfall for each pixel across KNP using the GRASS r.series algorithm in QGIS.

CHIRPS-based rainfall estimates were compared with daily observations from the only available rainfall gauge within KNP, located at the Bendili research station (est. July 2010; 0.56°N, 117.4°E; founded and operated by the Orangutan Kutai Project) in the NE corner of the park (Figure A2). It is important to note that this comparison serves to visualize conformity between datasets at a single location within KNP and that a standard validation analysis could not be performed without access to additional rainfall observations.

3. Results and Discussion

3.1. Forest Loss within KNP

Figure 2 depicts areas of baseline tree canopy cover (>30% coverage in 2000) and canopy loss throughout KNP between 2001–2021, as detected by the HGFC v1.9 dataset. Baseline canopy cover is shown in green and canopy loss is presented as an aggregate between 2001–2012 but annually thereafter (2013–2021) to reflect the greater detection accuracy of the post-2013 period (Figure 2). Much of the forest loss detected since 2000 is located along the trans-provincial highway that runs north-south through the eastern region of KNP (est. 1991) where illegal settlements and agricultural fields have proliferated over time. Outside of this highway region, notable patches of recent (dark blue) forest loss were also detected along the park's southern border (Figure 2A). The southwest patch borders an industrial tree plantation (oil palm and acacia) [34,35] while the easternmost patch borders an industrial open-pit coal mine [36].

To assess the validity of the HGFC estimates over KNP, we compared them with estimates from two other datasets for the years 2017–2020 over two sample areas of NE KNP (Figure 3). The three datasets conformed well in terms of the spatial pattern and area of canopy loss they detected over the two validation areas (Figure 3). Only two estimates by the reference dataset (in 2018 and 2020 over validation area B) were markedly different from those of the detection datasets (Figure 3)—perhaps an artifact of the different approaches that each use in the temporal detection of canopy loss (Figure A1). Overall, our validation supports the detection performance of the HGFC v1.9 dataset over this region, yet a standard validation analysis is warranted to quantify its accuracy over KNP.

The significant spike of canopy loss detected in 2016 (Figure 2C) coincides with the super El Niño drought of 2015–2016 that sparked major wildfires throughout the region according to Russon AE (pers. obs.) and [3,21]. Although this spike was detected in 2016, more than twice as many active fires and seven-times as much burned area were detected throughout KNP in 2015 than in 2016 (Figure 4). Since the HGFC dataset relies on clear-sky

observations for accurate detection, it is plausible that wildfire smoke and high cloud cover obscured most Landsat scenes during the 2015 fire season (August–November) so that most of the fire-related forest loss from 2015 could not be detected until the following year. This is one known caveat of the HGFC dataset, making it more useful in detecting multi-year trends in forest canopy loss than deriving definitive area estimates per year. Overall, the HGFC dataset detected 272 km^2 of total forest canopy loss between 2001–2021 (15% of the 2000 baseline canopy cover), half of which (137 km^2) was detected between 2015–2016. On average, the annual rate of loss within KNP during non-wildfire years between 2013–2021 was 5.6 km^2 (±1.3) per year, or a loss of 0.3% of baseline forest cover each year.

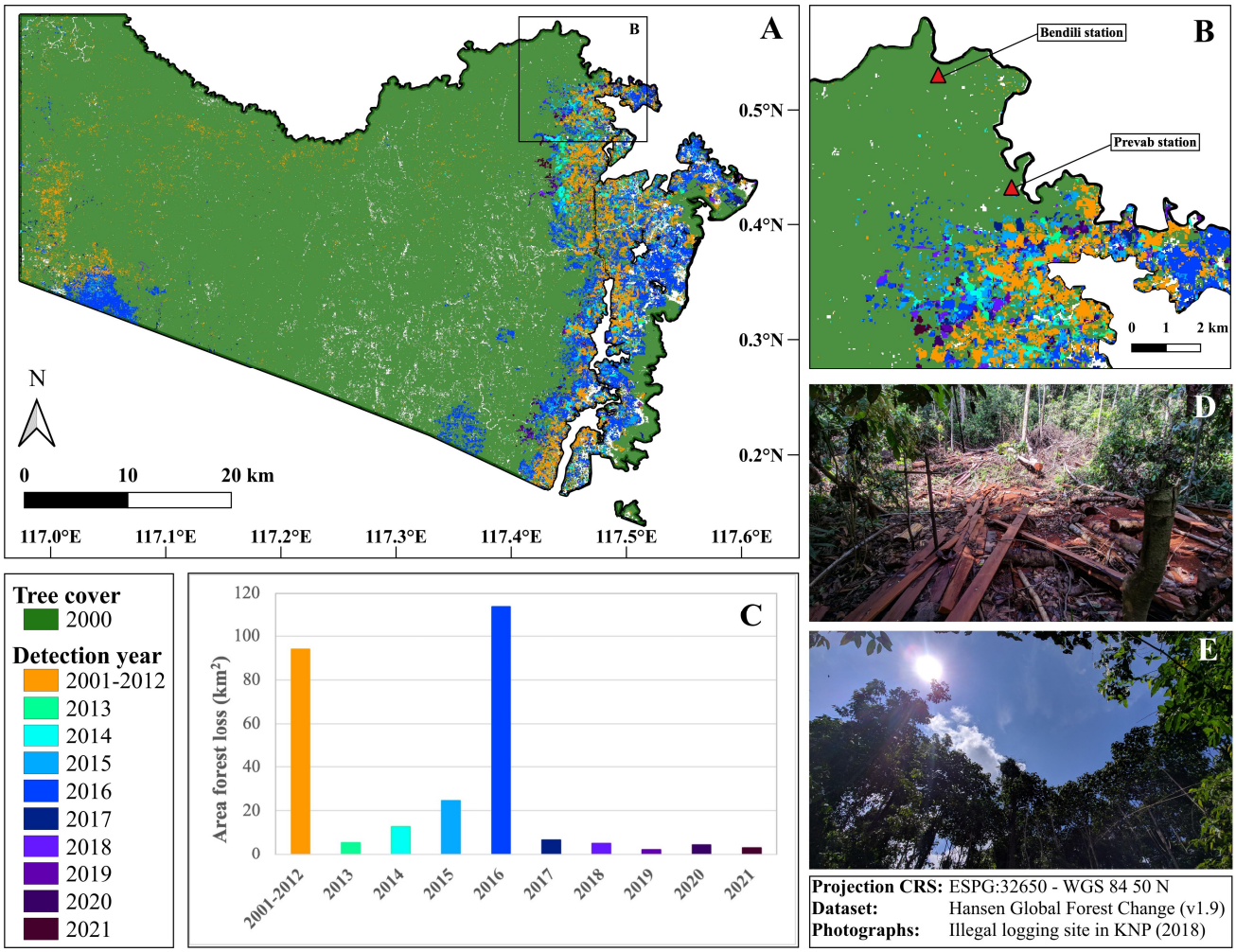

Figure 2. Classified areas of forest loss within Kutai National Park (**A**) and the Greater Mentoko Area [GMA] (**B**) between 2001–2021 and corresponding area estimates (**C**) as detected by the Hansen Global Forest Change (v1.9) dataset. Only years post-2013 are discretized annually due to higher detection accuracy of the 2013–2021 period. Tree cover with >70% canopy closure in year 2000 are depicted in green. Images of an illegal logging site (**D**) and the resultant canopy opening (**E**) in the GMA from 2018 by RG.

The only area of KNP for which accounts of pre-disturbance forest conditions are available is the Greater Mentoko Area (GMA) of NE KNP (Figure 2B). As the site of the first orangutan research in Indonesia in 1970 [37], its forests were described as "near-pristine", free of major logging activities, and only affected by natural disturbances such as wind-throws, droughts, and recurrent river flooding [38,39]. Since 2000, nearly half of its original forest cover has been lost (Figure 2B) to both fire- and non-fire disturbances, the latter of which include illegal logging, settlements, and agricultural expansion to support the local

population (Sangatta) that has grown 500-fold over the past five decades [6]. Attributing precise contributions of fire- and non-fire disturbances to annual forest loss within KNP, however, requires further analysis beyond the scope of this study.

The forest loss detected in the GMA has replaced primary habitat for the resident orangutans in this area (est. 1000 individuals) [9] and placed their home ranges in closer proximity to humans and their livelihoods—exacerbating the record-setting rates of human-orangutan conflict reported within KNP [40,41]. Further loss in this region along a westward trajectory will also have negative implications for the local human population by weakening crucial forest-related ecosystem services (e.g., flood management, water quality, climate regulation, availability of non-timber forest products, etc.) and by compromising park tourism that relies in large part on the forested orangutan habitats around the Prevab research station (Figure 2B).

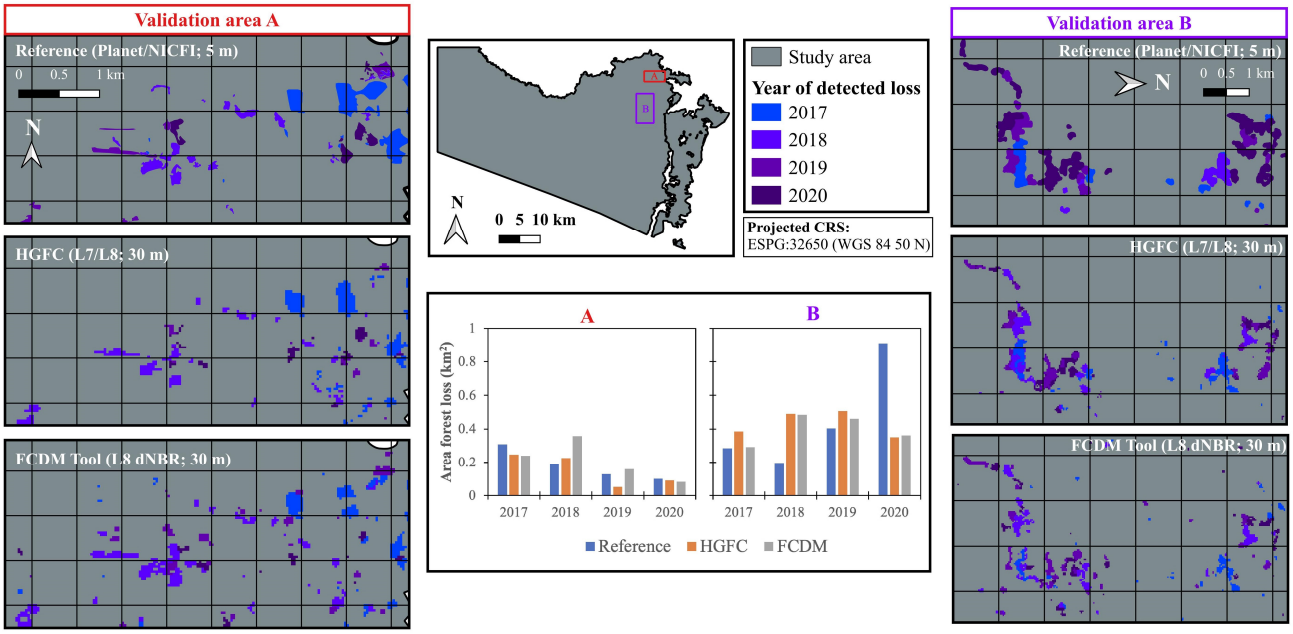

Figure 3. Validation of the Hansen Global Forest Change (HGFC; v1.9) product for the years 2017–2020 over two sample regions (**A**,**B**) in northeastern KNP using (1) high-resolution Planet/NICFI satellite imagery (Reference dataset) and (2) the Forest Canopy Disturbance Monitoring Tool (FCDM Tool) developed by [26].

3.2. Hotspot Mapping within KNP

Between 2002–2021, a significant amount of BA was detected throughout KNP in 2004, 2015, and 2016 by the MCD64A1 dataset (Figure 4). The BA from 2015 cover settlement areas and agricultural fields in NE KNP and coincides with recently disturbed forests in SW KNP that had lost canopy cover only a year prior (Figures 2A and 4A). Date-of-burning estimates suggest that fires (2015) in the latter region spread from the neighbouring industrial plantation into the recently disturbed area, resulting in a footprint of burning that dwarfs the patches of earlier (2014) forest loss (Figures 2A and 4A). The effect of recent canopy openings facilitating the spread and development of wildfires that cause further deforestation has been well documented in past studies in this region [42,43].

AF observations (VIIRS) revealed a significant footprint of fires in eastern KNP between 2015–2016 that coincide with detected forest loss over this period (Figure 2) but not with BA (Figure 4D). This is perhaps because relative to BA datasets, AF products are known to detect more small-scale fires [28], such as those originating from the individual smallholder farms that predominate eastern KNP. Lower detection accuracy over croplands and other areas of predominantly small fires is a known limitation of the MCD64A1 dataset, owing largely to its coarse resolution (500 m) [27,28,44].

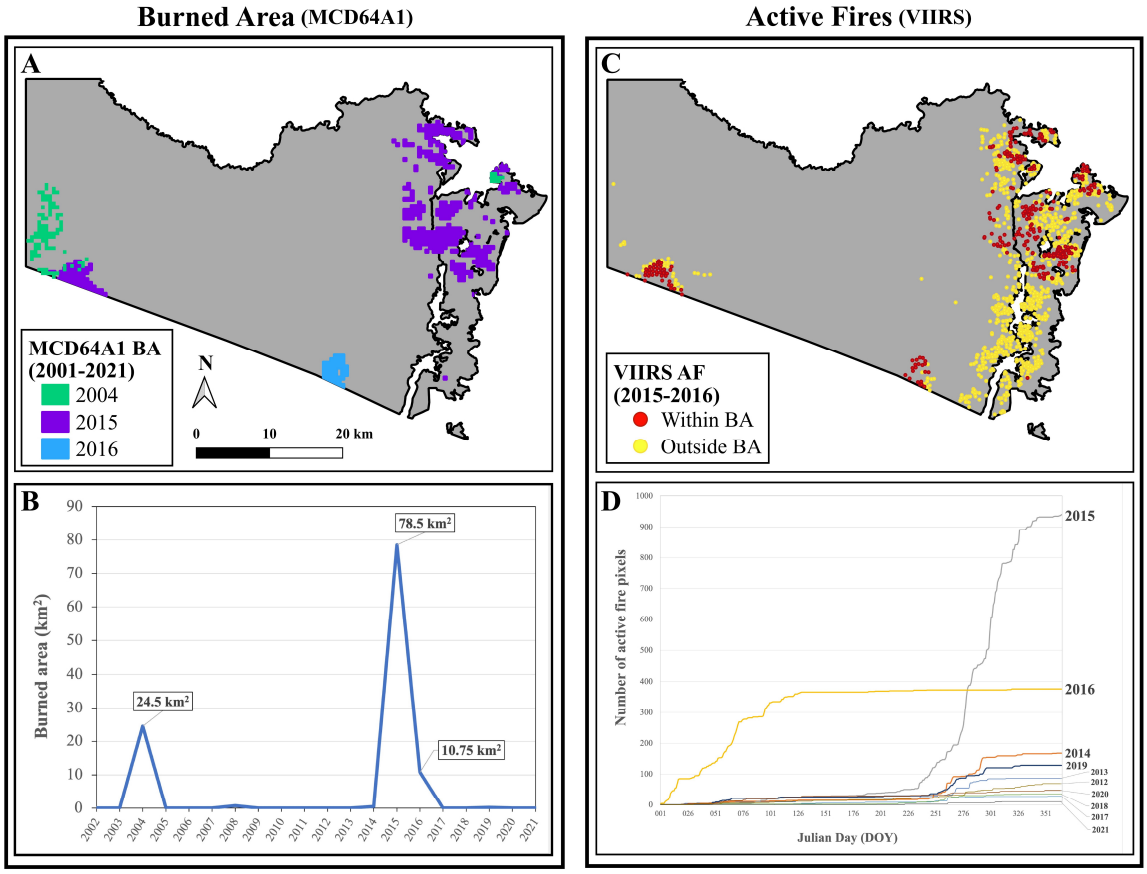

Figure 4. MCD64A1 (left): location (**A**) and annual estimates (**B**) of detected burned area (BA) within KNP between 2002–2021. VIIRS (right): active fire detections within and outside the perimeters of detected BA in KNP between 2015–2016 (**C**) and cumulative active fire detections across days of the year (DOY) between 2012–2021 within KNP (**D**).

To further assess the validity of MCD64A1-detected BA over KNP, we followed a validation approach defined by UN-SPIDER that maps burn severity using the difference of normalized burn ratios (dNBR) between pre- and post-fire satellite images (Figure 5). We chose to validate BA from the 2015 wildfires using L8 cloud-free composite images over three sample areas of KNP, covering both burned (regions A and C) and non-burned (region B) land according to MCD64A1 (Figure 5; see caveats in Section 2.2.2). The MCD64A1 dataset performed well over the SW region of KNP where croplands are absent, but poorly over the other sampled areas where croplands predominate; it missed all of the moderate- to severe-burn scars over SE KNP (Figure 5) despite a large number of active fire detections over this region in 2015 (Figure 4). Despite its poor performance over croplands, the MCD64A1 dataset still provides a good indicator of years of high BA within KNP (Figure 4), but alternative BA datasets and/or mapping methods are required to estimate the contributions of fire to forest loss in this region.

3.3. Climatic Influences of Fire and Forest Loss within KNP

According to estimates of total "fire season" (Aug–Nov) rainfall over the past 25 years, the deforested eastern region of the park receives the least amount of rainfall, as low as 5.5 mm/day (500 mm/3 mo.) on average around the bounds of Sangatta city (Figure 6A). Previous research over Borneo and other tropical regions has found patterns of lower rainfall and higher ambient temperatures over deforested areas (compared to unlogged), with the most pronounced effects observed during the dry season and El Niño-related droughts [45,46]. Deforested areas are also more accessible to humans, experience higher temperature extremes, and contain relatively higher fuel loads from logging debris and

woody successional plants, all of which contribute to an elevated fire hazard/risk in such areas [43,47]. These implications are supported by studies that have connected rampant deforestation patterns throughout eastern Borneo with stronger El Niño droughts [45,47] and more severe and widespread wildfires [42].

During the 2015 fire season, rainfall estimates (<2.5 mm/day) and single-point observations (<0.75 mm/day) reveal extreme drought conditions over much of the burned area (Figure 6B), well below the reported 4–5 mm/day fire risk threshold for this region [3,45]. These severe drought conditions—driven by a 20-year peak of El Niño strength—combined with a prevalence of potential ignition sources (see [6]) and widespread degradation to facilitate large-scale wildfires within KNP (Figure 7). It is likely that such wildfires contributed both directly (i.e., drought- and fire-related mortality) and indirectly (i.e., facilitating clearing/conversion) to the spike in detected forest loss over this period (Figure 7), but further analysis is necessary to confirm this interpretation.

Rainfall estimates also suggest that most—but not all—of the six El Niño events over the past 20 years have induced drought conditions below the fire risk threshold for this region (Figure 7). Spikes in BA were only detected during one weak (2004–2005) and one strong (2015–2016) EN event, but none were detected during several moderate-strength EN events that induced comparable rainfall deficits (Figure 7). Assuming that the MCD64A1 dataset is a sufficient indicator of large-scale fire occurrences within KNP, we posit that other factors, such as temperature and the incidental presence of ignition sources, have regulated the intensity and spread of fire throughout KNP during severe droughts. However, ongoing deforestation in KNP and predictions of more frequent and extreme super El Niño events [48–51] will worsen the fire hazard of this reserve during future droughts.

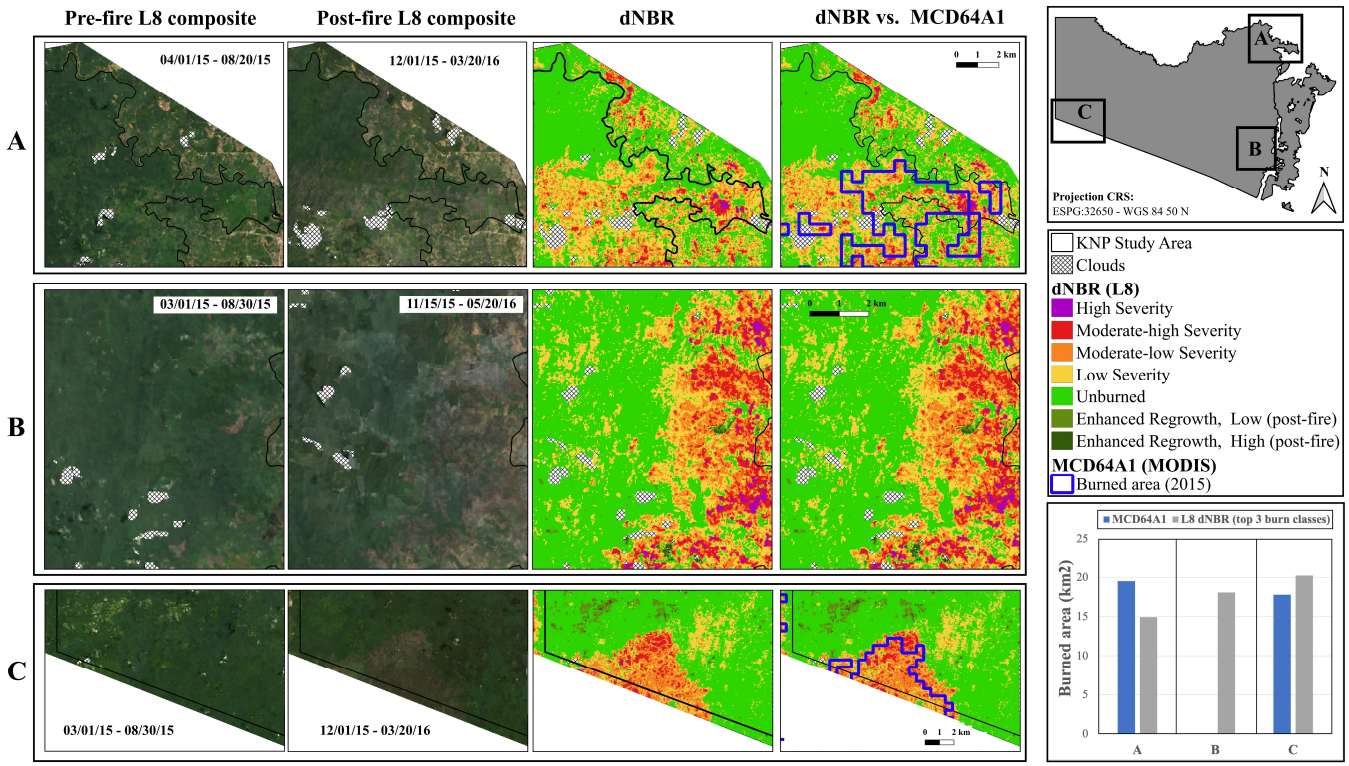

Figure 5. Validation of MCD64A1 burned area in 2015 over northwestern (**A**), southeastern (**B**), and southwestern (**C**) sample regions of Kutai National Park using differenced normalized burn ratio (dNBR) of pre- and post-fire Landsat 8 composite imagery. In the bottom right chart, the spatial extent of the MCD64A1-detected burned areas is compared against the top three classes of dNBR burn severity over each sample region.

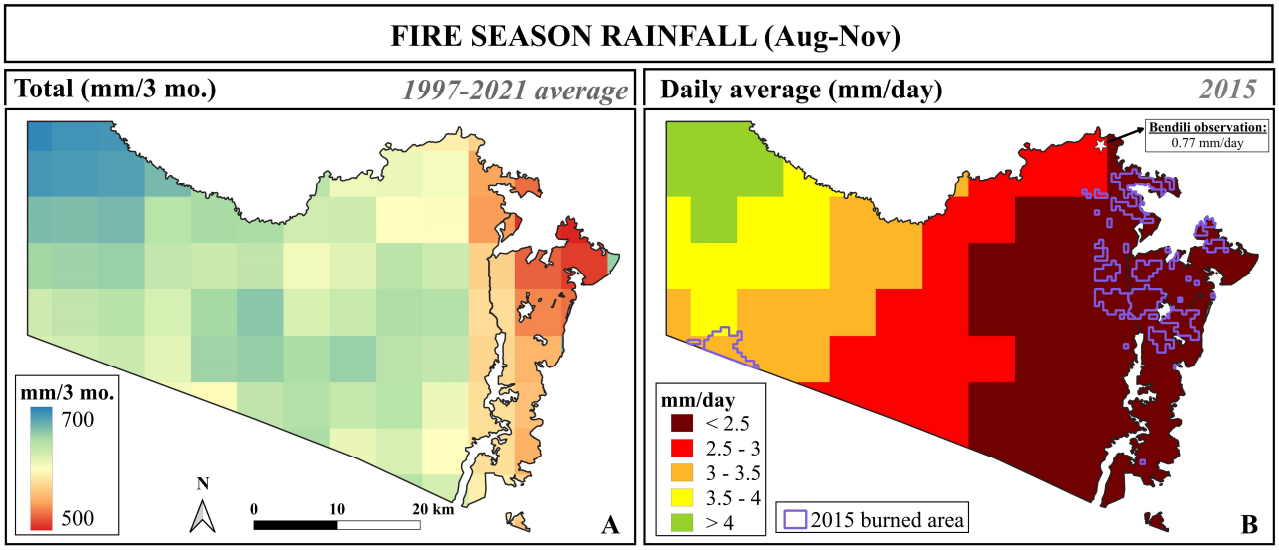

Figure 6. Per-pixel averages (1997–2021) of total rainfall (**A**) and daily average rainfall vs. burned area in 2015 (**B**) during the standard fire season (August–November) within Kutai National Park. Rainfall estimates from CHIRPS Pentad; burned area estimates from MCD64A1.

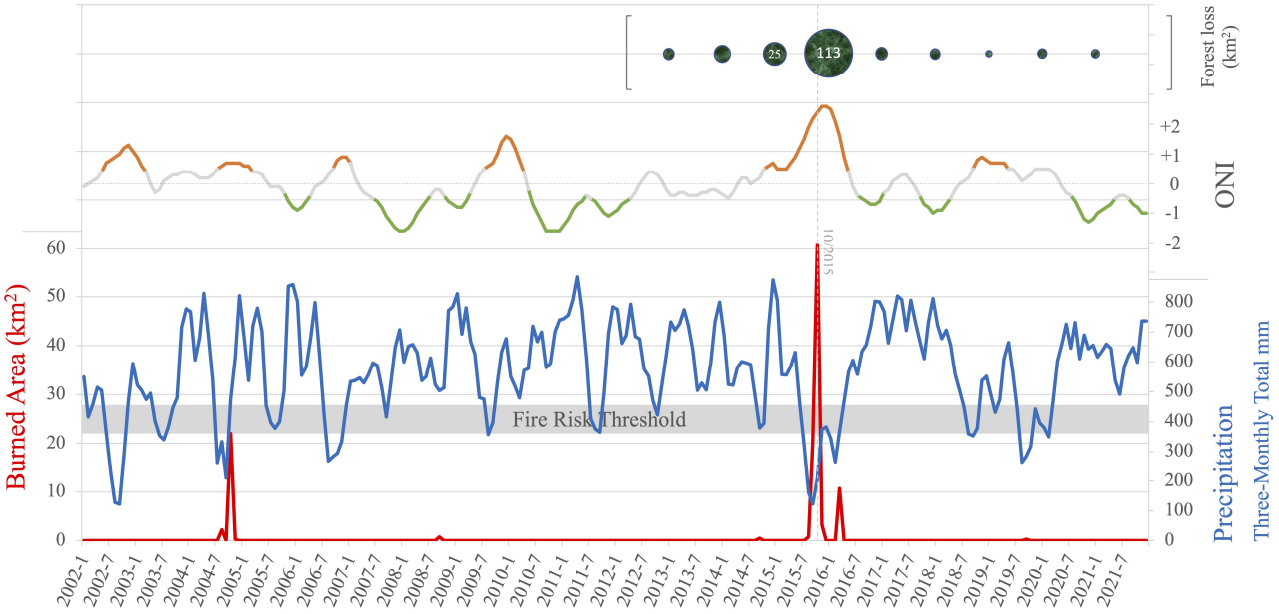

Figure 7. Estimates of monthly burned area (MCD64A1) and three-monthly total precipitation (CHIRPS) within Kutai National Park, as well as the Oceanic Niño Index (ONI) between 2002–2021, with phases of El Niño in orange and La Niña in green. Green bubbles (top) represent annual estimates of forest loss within KNP (HGFC v1.9) between 2013–2021 in square kilometers (aligned to Jan 1 of the detection year). The reported fire risk threshold for this region of 4–5 mm/day (360–450 mm/3 month period) is denoted by the grey band.

4. Conclusions

In this study, we leveraged the extensive collection of historical satellite data and the processing power of Google Earth Engine to investigate trends in and influences on forest loss within Indonesia's Kutai National Park over various time frames since 1997. We found a gradual yet considerable westward progression of forest loss across the eastern (settled/farmed) region of KNP since 2000 and patches of fire-related forest loss along the park's southern border associated with the El Niño-related drought and fires of 2015–2016. In total, the HGFC v1.9 dataset detected 272 km^2 of forest loss (or 15% of baseline forest

cover) since 2000, half of which (137 km^2) occurred between 2015–2016 with significant overlap of detected burn scars. Our validation analyses support the detection performance of the HGFC v1.9 over NE KNP but they caution the use of the MCD64A1 burned area dataset over eastern KNP where considerable croplands compromise its accuracy. Our analysis of rainfall estimates also suggests that most El Niño events since 2000 have induced prolonged droughts over KNP below the fire risk threshold (4–5 mm/day) for this region. However, we found that drought severity alone cannot explain fire intensity within KNP, indicating the influences of other modulating factors (e.g., anomalous temperatures, incidental presence of fire sources, recent logging) in this phenomenon. Unlike all other areas of KNP, its eastern settled/farmed region receives average rainfall amounts that approach the fire risk threshold during the standard fire season (August–November), which is potentially (in part) attributable to widespread deforestation as demonstrated elsewhere in Borneo (Chapman et al. 2020; McAlpine et al. 2018). Lastly, we found that the most intense wildfire event of the past two decades—in 2015—coincided with rainfall estimates of <2.5 mm/day over the most fire-affected areas of the park.

Limitations of our analyses include the use of composite imaging in our validation assessments to address the obstacle of high-cloud cover over KNP. With this approach, we were still able to detect clear signals of canopy openings and burn scars in our validation analyses, thus adding confidence to our discussion of forest loss and its relative contributions over our study area. However, precise contributions of fire- and non-fire disturbances to annual forest loss within KNP could not be estimated with our approach, which along with standard validation assessments of the datasets used, should be the subject of future studies within KNP. Future studies of fire dynamics over KNP should also examine mechanisms of fire spread during wildfire years to identify targets of fire management efforts in this region.

The rates and influences of forest loss reported here contribute to undermining tourism-related revenue, degrading essential ecosystem services, heightening fire risk and severity in the region, and threatening the considerable biodiversity that resides within the park, including a stronghold population of the critically endangered Northeast Bornean orangutan. With the relocation of the Indonesian government capital to East Kalimantan scheduled for 2024, unprecedented new human migration into East Kalimantan and subsequent land and building requirements are soon likely to exert added pressures on KNP's forests. Wildfires and illegal logging within KNP must therefore be the priority subject of future conservation, management, and research programs to avoid further loss of forest cover in this protected area.

Author Contributions: Conceptualization, R.G.; formal analysis, R.G.; funding acquisition, X.W.; methodology, R.G.; resources, A.E.R.; supervision, X.W.; writing—original draft, R.G.; writing—review and editing, X.W. and A.E.R. All authors have read and agreed to the published version of the manuscript.

Funding: This research was supported by the Natural Science and Engineering Research Council of Canada and the New Frontiers in Research Fund.

Data Availability Statement: The source codes for the Google Earth Engine scripts used in this paper are available at: https://github.com/ryan-guild/Kutai-National-Park-Deforestation-Fire-Rainfall-Mapping-Study.git. The Hansen Global Forest Change v1.9 dataset is available at: https://developers.google.com/earth-engine/datasets/catalog/UMD_hansen_global_forest_change_2021_v1_9 (accessed on 1 September 2022). The MCD64A1.061 MODIS dataset is available at: https://developers.google.com/earth-engine/datasets/catalog/MODIS_061_MCD64A1 (accessed on 1 September 2022). The CHIRPS Pentad dataset is available at: https://developers.google.com/earth-engine/datasets/catalog/UCSB-CHG_CHIRPS_PENTAD?hl=en (accessed on 1 September 2022).

Conflicts of Interest: The authors declare no conflict of interest.

Appendix A

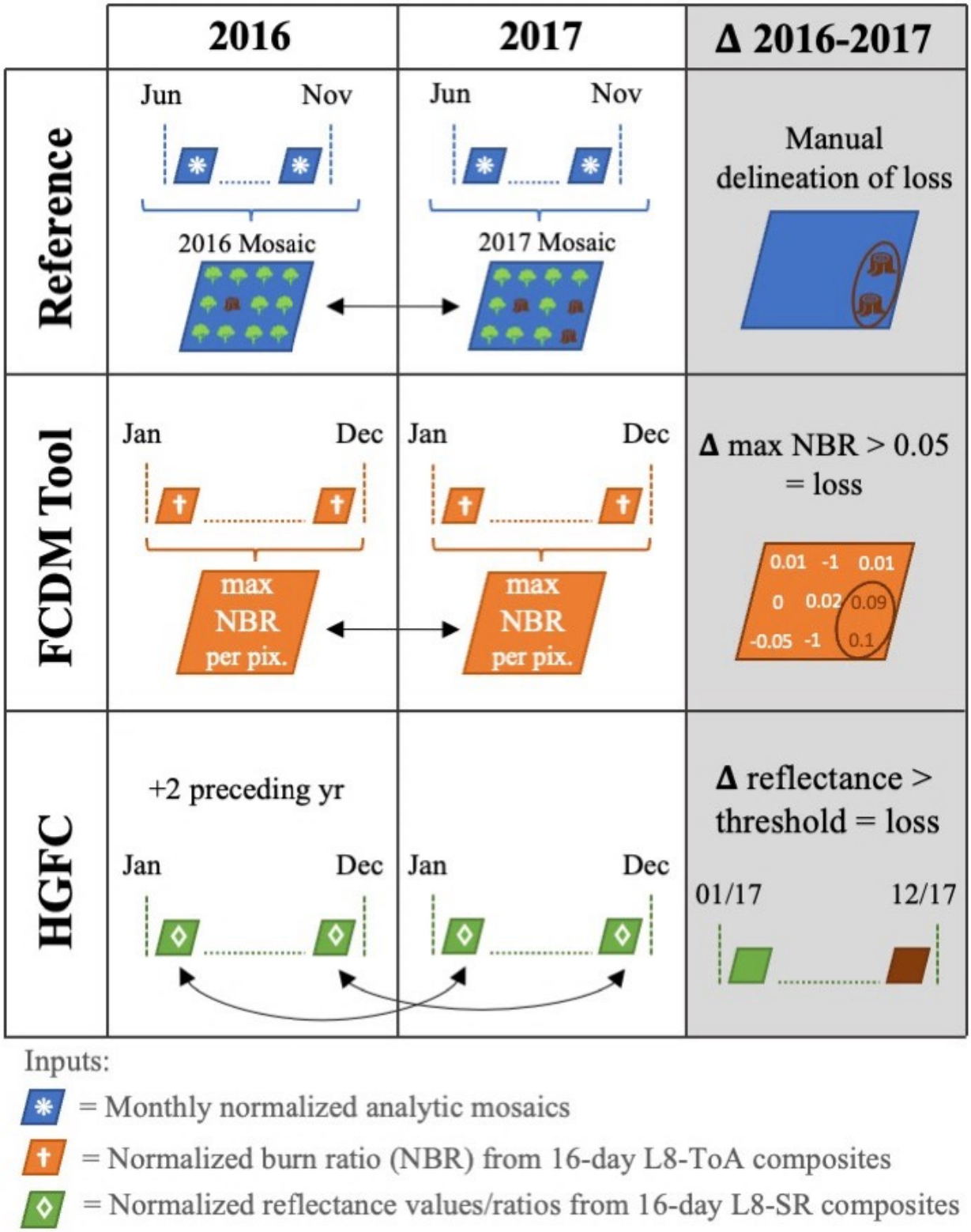

Figure A1. Differences in detection methodology between the three forest loss datasets used in this study, including the reference dataset (Planet/NICFI imagery), FCDM Tool [26], and the Hansen Global Forest Change product [23].

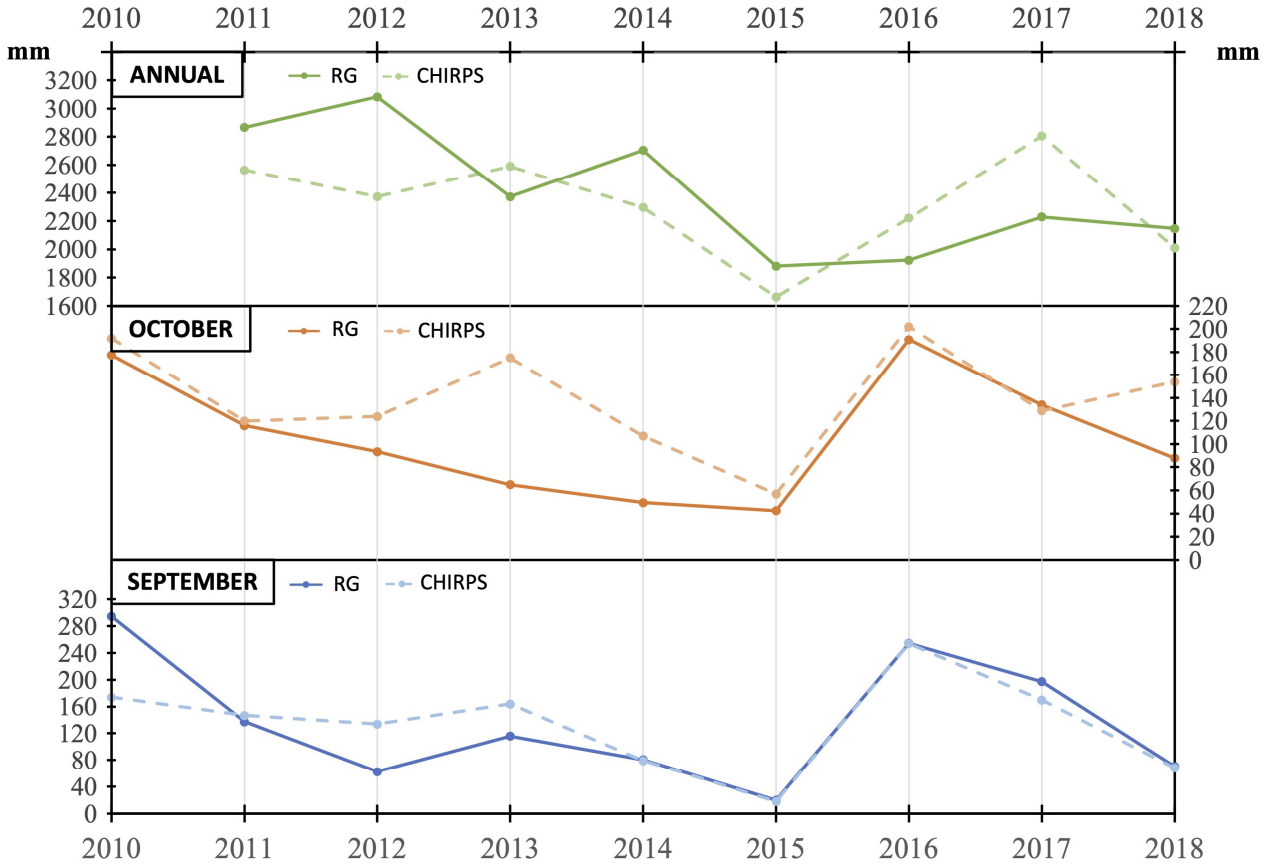

Figure A2. Comparison of rainfall estimates (CHIRPS) and rain gauge observations (RG) at the Bendili research station in Kutai National Park for annual, September, and October time periods between 2010–2018. Bendili RG observations are courtesy of the Orangutan Kutai Project.

References

1. Soehartono, T.; Mardiastuti, A. *The voice of National Parks in Kalimantan, Indonesia: Searching the Truth of Thirty Year National Park Development*; Nata Samastha Foundation: Bogor, Indonesia, 2013; p. 244.
2. Utami-Atmoko, S.; Traylor-Holzer, K.; Rifqi, M.A.; Siregar, P.G.; Achmad, B.; Priadjati, A.; Husson, S.; Wich, S.; Hadisiswoyo, P.; Saputra, F.; et al. *Orangutan Population and Habitat Viability Assessment: Final Report*; IUCN/SSC Conservation Breeding Specialist Group: Bogor, Indonesia, 2017; p. 121.
3. Field, R.D.; van der Werf, G.R.; Fanin, T.; Fetzer, E.J.; Fuller, R.; Jethva, H.; Levy, R.; Livesey, N.J.; Luo, M.; Torres, O.; et al. Indonesian fire activity and smoke pollution in 2015 show persistent nonlinear sensitivity to El Niño-induced drought. *Proc. Natl. Acad. Sci. USA* **2016**, *113*, 9204–9209. [CrossRef] [PubMed]
4. Siegert, F.; Hoffmann, A.A. The 1998 forest fires in East Kalimantan (Indonesia): A quantitative evaluation using high resolution, mulitemporal ERS-2 SAR Images and NOAA-AVHRR hotspot data. *Remote Sens. Environ.* **2000**, *72*, 64–77. [CrossRef]
5. Hadiprakarsa, Y.Y.; Rianta, E.; Christy, L.; Siregar, P.; Kitchener, D.; Hartman, P. *PSSF (Private Sector Sustainability Facility) Site Threats: Evaluation of Threats to Orangutan and Priority Interventions to Abate These Threats at PSSF Focused Sites in North Sumatra and East Kalimantan*; Report for the United States Agency for International Development (USAID); USAID: Washington, DC, USA, 2009; 32p.
6. Guild, R. Threats to wild orangutans: A case study in Kutai National Park of East Kalimantan, Indonesia. Master's Thesis, York University, Toronto, ON, Canada, 2019; p. 79.
7. Ustin, S.L.; Middleton, E.M. Current and near-term advances in Earth observation for ecological applications. *Ecol. Process.* **2021**, *10*, 1–57. [CrossRef] [PubMed]
8. Hasanah, N.I. Perubahan penutupan lahan di Taman Nasional Kutai provinsi Kalimantan Timur (Land cover change in Kutai National Park of East Kalimantan province). Ph.D. Thesis, Bogor Agricultural University, Bogor City, Indonesia, 2011; p. 68.
9. BTNK (Balai Taman National Kutai). *Statistik Taman Nasional Kutai: Tahun 2017 (Kutai National Park Statistics: 2017)*; BTNK (Balai Taman National Kutai): Bontang, Indonesia, 2017; p. 135.
10. BTNK (Balai Taman National Kutai). *Statistik Taman Nasional Kutai: Tahun 2016*; BTNK (Balai Taman National Kutai): Bontang, Indonesia, 2016; p. 173.

11. Rist, L.; Feintrenie, L.; Levang, P. The livelihood impacts of oil palm: Smallholders in Indonesia. *Biodivers. Conserv.* **2010**, *19*, 1009–1024. [CrossRef]
12. Cahyadi, E.R.; Waibel, H. Contract farming and vulnerability to poverty among oil palm smallholders in Indonesia. *J. Dev. Stud.* **2016**, *52*, 681–695. [CrossRef]
13. Naylor, R.L.; Higgins, M.M.; Edwards, R.B.; Falcon, W.P. Decentralization and the environment: Assessing smallholder oil palm development in Indonesia. *Ambio* **2019**, *48*, 1195–1208. [CrossRef]
14. Schweithelm, J.; Glover, D. Causes and impacts of the fires. In *Indonesia's Fires and Haze: The Cost of Catastrophe*; Glover, D., Jessup, T., Eds.; Institute of Southeast Asian Studies: Singapore, Singapore, 2006; pp. 1–13.
15. Goldammer, J.G. Natural rain forest fires in eastern Borneo during the Pleistocene and Holocene. *Naturwissenschaften* **1989**, *76*, 518–520. [CrossRef]
16. Wirawan, N. *Kutai National Park Management Plan 1985–1990*; World Wildlife Fund (WWF): Bogor, Indonesia, 1985.
17. Leighton, M.; Wirawan, N. Catastrophic drought and fire in Bornean tropical rain forest associated with the 1982–1983 ENSO event. In *Tropical Rain Forests and the World Atmosphere*; Prance, G., Ed.; Westview Press: Boulder, CO, USA, 1986; pp. 75–102.
18. Mori, T. Effects of droughts and forest fires on dipterocarp forests in East Kalimantan. In *Rainforest Ecosystems of East Kalimantan*; Guhardja, E., Fatawi, M., Sutisna, M., Mori, T., Ohta, S., Eds.; Springer: Tokyo, Japan, 2000; pp. 29–42.
19. Slik, J.F.W.; Verburg, R.W.; Keßler, P.J.A. Effects of fire and selective logging on tree species composition of lowland dipterocarp forest in East Kalimantan, Indonesia. *Biodivers. Conserv.* **2002**, *11*, 85–98. [CrossRef]
20. Russon, A.E.; Kuncoro, P.; Ferisa, A. Orangutan behavior in Kutai National Park after drought and fire damage: Adjustments to short- and long-term natural forest regeneration. *Am. J. Primatol.* **2015**, *77*, 1276–1289. [CrossRef]
21. Pan, X.; Chin, M.; Ichoku, C.M.; Field, R.D. Connecting Indonesian fires and drought with the type of El Niño and phase of the Indian Ocean Dipole during 1979–2016. *J. Geophisical Res. Atmos.* **2018**, *123*, 7974–7988.
22. Schiavina, M.; Freire, S.; MacManus, K. GHS-POP R2019A—GHS Population Grid Multitemporal (1975–1990–2000–2015). European Commission, Joint Research Centre (JRC) [Dataset]. 2019. Available online: https://doi.org/10.2905/0C6B9751-A71F-4062-830B-43C9F432370F (accessed on 18 September 2022).
23. Hansen, M.C.; Potapov, P.V.; Moore, R.; Hancher, M.; Turubanova, S.A.; Tyukavina, A.; Thau, D.; Stehman, S.V.; Goetz, S.J.; Loveland, T.R.; et al. High-resolution global maps of 21st-century forest cover change. *Science* **2013**, *342*, 850–853. [CrossRef] [PubMed]
24. Potapov, P.; Hansen, M.C.; Kommareddy, I.; Kommareddy, A.; Turubanova, S.; Pickens, A.; Adusei, B.; Tyukavina, A.; Ying, Q. Landsat analysis ready data for global land cover and land cover change mapping. *Remote Sens.* **2020**, *12*, 426. [CrossRef]
25. Potapov, P.; Tyukavina, A.; Turubanova, S.; Talero, Y.; Hernandez-Serna, A.; Hansen, M.; Saah, D.; Tenneson, K.; Poortinga, A.; Aekakkararungroj, A.; et al. Annual continuous fields of woody vegetation structure in the Lower Mekong region from 2000-2017 Landsat time-series. *Remote Sens. Environ.* **2019**, *232*, 111278. [CrossRef]
26. Langner, A.; Miettinen, J.; Kukkonen, M.; Vancutsem, C.; Simonetti, D.; Vieilledent, G.; Verhegghen, A.; Gallego, J.; Stibig, H.-J. Towards Operational Monitoring of Forest Canopy Disturbance in Evergreen Rain Forests: A Test Case in Continental Southeast Asia. *Remote Sens.* **2018**, *10*, 544. [CrossRef]
27. Giglio, L.; Boschetti, L.; Roy, D.P.; Humber, M.L.; Justice, C.O. The collection 6 MODIS burned area mapping algorithm and product. *Remote Sens. Environ.* **2018**, *217*, 72–85. [CrossRef]
28. Hall, J.V.; Argueta, F.; Giglio, L. Validation of MCD64A1 and FireCCI51 cropland burned area mapping in Ukraine. *Int. J. Appl. Earth Obs. Geoinf.* **2021**, *102*, 102443. [CrossRef]
29. Katagis, T.; Gitas, I.Z. Assessing the Accuracy of MODIS MCD64A1 C6 and FireCCI51 Burned Area Products in Mediterranean Ecosystems. *Remote Sens.* **2022**, *14*, 602. [CrossRef]
30. Liu, T.; Marlier, M.E.; Karambelas, A.; Jain, M.; Singh, S.; Singh, M.K.; Gautam, R.; DeFries, R.S. Missing emissions from post-monsoon agricultural fires in northwestern India: Regional limitations of MODIS burned area and active fire products. *Environ. Res. Commun.* **2019**, *1*, 011007. [CrossRef]
31. Liu, T.; Mickley, L.J.; Marlier, M.E.; DeFries, R.S.; Khan, M.F.; Latif, M.T.; Karambelas, A. Diagnosing spatial biases and uncertainties in global fire emissions inventories: Indonesia as regional case study. *Remote. Sens. Environ.* **2020**, *237*, 111557. [CrossRef]
32. Funk, C.; Peterson, P.; Landsfeld, M.; Pedreros, D.; Verdin, J.; Shukla, S.; Husak, G.; Rowland, J.; Harrison, L.; Hoell, A.; et al. The climate hazards infrared precipitation with stations—A new environmental record for monitoring extremes. *Sci. Data* **2015**, *2*, 150066. [CrossRef]
33. Sloan, S.; Tacconi, L.; Cattau, M.E. Fire prevention in managed landscapes: Recent success and challenges in Indonesia. *Mitig. Adapt. Strat. Glob. Chang.* **2021**, *26*, 1–30. [CrossRef]
34. Petersen, R.; Askenov, D.; Esipova, E.; Goldman, E.; Harris, N.; Kuksina, N.; Kurakina, I.; Loboda, T.; Manisha, A.; Sargent, S.; et al. *Mapping Tree Plantations with Multispectral Imagery: Preliminary Results for Seven Tropical Countries*; World Resources Institute: Washington, DC, USA, 2016; p. 18.
35. Runting, R.K.; Ruslandi Griscom, B.; Struebig, M.J.; Satar, M.; Meijaard, E.; Burivalova, Z.; Cheyne, S.M.; Deere, N.J.; Game, E.T.; Putz, F.E.; et al. Larger gains from improved management over sparing-sharing for tropical forests. *Nat. Sustain.* **2019**, *2*, 53–61. [CrossRef]

36. Ministry of Energy and Natural Resources Indonesia. "ESDM One Map Indonesia". 2022. Available online: https://geoportal.esdm.go.id/minerba/ (accessed on 20 September 2022).
37. Rodman, P.S. Synecology of Bornean primates: With special reference to the behavior and ecology of orangutans. Ph.D. Thesis, Harvard University, Cambridge, MA, USA, 1973; p. 218.
38. Leighton, M. Fruit Resources and Patterns of Feeding, Spacing and Grouping Among Sympatric Bornean hornbills (*Bucerotidae*). Ph.D. Thesis, University of California, Davis, CA, USA, 1982.
39. Wilson, C.C.; Wilson, W.L. The influence of selective logging on primates and some other animals in East Kalimantan. *Folia Primatol.* **1975**, *23*, 245–274. [CrossRef] [PubMed]
40. Meijaard, E.; Buchori, D.; Hadiprakarsa, Y.; Utami-Atmoko, S.S.; Nurcahyo, A.; Tiju, A.; Prasetyo, D.; Nardiyono; Christie, L.; Ancrenaz, M.; et al. Quantifying killing of orangutans and human-orangutan conflict in Kalimantan, Indonesia. *PLoS ONE* **2011**, *6*, e27491. [CrossRef] [PubMed]
41. Abram, N.K.; Meijaard, E.; Wells, J.A.; Ancrenaz, M.; Pellier, A.S.; Runting, R.K.; Gaveau, D.; Wich, S.; Nardiyono; Tiju, A.; et al. Mapping perceptions of species' threats and population trends to inform conservation efforts: The Bornean orangutan case study. *Divers. Distrib.* **2015**, *21*, 487–499. [CrossRef]
42. Siegert, F.; Ruecker, G.; Hinrichs, A.; Hoffmann, A.A. Increased damage from fires in logged forests during droughts caused by El Niño. *Lett. Nat.* **2001**, *414*, 437–440. [CrossRef]
43. Van Nieuwstadt, M.G.L.; Sheil, D. Drought, fire and tree survival in a Borneo rain forest, East Kalimantan, Indoensia. *J. Ecol.* **2005**, *93*, 191–201. [CrossRef]
44. Zhang, T.; Wooster, M.J.; de Jong, M.; Xu, W. How well does the "small fire boost" methodology used within the GFED4.1s fire emissions database represent the timing, location and magnitude of agricultural burning? *Remote Sens.* **2018**, *10*, 823. [CrossRef]
45. Chapman, S.; Syktus, J.; Trancoso, R.; Salazar, A.; Thatcher, M.; Watson, J.E.M.; Meijaard, E.; Sheil, D.; Dargusch, P.; McAlpine, C.A. Compounding impact of deforestation on Borneo's climate during El Niño events. *Environ. Res. Lett.* **2020**, *15*, 084006. [CrossRef]
46. Perugini, L.; Caporaso, L.; Marconi, S.; Cescatti, A.; Quesada, B.; De Noblet, N.; House, J.I.; Arneth, A. Biophysical effects on temperature and precipitation due to land cover change. *Environ. Res. Lett.* **2017**, *12*, 1–13. [CrossRef]
47. McAlpine, C.A.; Johnson, A.; Salazar, A.; Syktus, J.; Wilson, K.; Meijaard, E.; Seabrook, L.; Dargusch, P.; Nordin, H.; Sheil, D. Forest loss and Borneo's climate. *Environ. Res. Lett.* **2018**, *13*, 044009. [CrossRef]
48. Cai, W.; Borlace, S.; Lengaigne, M.; van Rensch, P.; Collins, M.; Vecchi, G.; Timmermann, A.; Santoso, A.; McPhaden, M.J.; Wu, L.; et al. Increasing frequency of extreme El Niño events due to greenhouse warming. *Nat. Clim. Change* **2014**, *4*, 111–116. [CrossRef]
49. Cai, W.; Wang, G.; Dewitte, B.; Wu, L.; Santoso, A.; Takahashi, K.; Yang, Y.; Carréric, A.; McPhaden, M.J. Increased variability of eastern Pacific El Niño under greenhouse warming. *Nature* **2018**, *564*, 201–206. [CrossRef] [PubMed]
50. Chen, C.C.; Lin, H.W.; Yu, J.Y.; Lo, M.H. The 2015 Borneo Fires: What have we learned from the 1997 and 2006 El Niños? *Environ. Res. Lett.* **2016**, *11*, 104003. [CrossRef]
51. Wang, B.; Luo, X.; Yang, Y.M.; Sun, W.; Cane, M.A.; Cai, W.; Yeh, S.W.; Liu, J. Historical changes of El Niño properties sheds light on future changes of extreme El Niño. *Proc. Natl. Acad. Sci. USA* **2019**, *116*, 22512–22517. [CrossRef]